Title:

IntelliProfiler: a novel software pipeline for analyzing multiple animals with a high-resolution home-cage RFID system

Authors: Shohei Ochi[1*], Hitoshi Inada[1,2], Noriko Osumi[1*]

Affiliation:

[1] Department of Developmental Neuroscience, Tohoku University Graduate School of Medicine, Sendai, Miyagi 980-8575, Japan

[2] Department of Biochemistry and Cellular Biology, National Institute of Neuroscience, NCNP, Kodaira, Tokyo, Japan.

*Correspondence: noriko.osumi.c7@tohoku.ac.jp and shohei.ochi.a5@tohoku.ac.jp

Abstract

There is an increasing need for unbiased behavioral analysis systems that accommodate multi-animal interactions in semi-natural environments. Here we present "IntelliProfiler," a software pipeline designed to analyze locomotor activity and social proximity using a commercially available, previously validated radio frequency identification (RFID) floor array. IntelliProfiler can track and analyze up to 16 mice simultaneously, enabling long-term assessment of both locomotor and social behaviors over extended periods. Using this system, we found that male mice tend to maintain greater social distances than females, and that group size critically influences male social network dynamics. Furthermore, aging significantly affected both locomotor activity and social interaction in a group size-dependent manner. Additionally, a mouse model of autism spectrum disorder (ASD) derived from aged fathers exhibited hyperactivity and increased social distance compared to controls, indicating altered patterns of social interaction, an ASD-related phenotype. These findings demonstrate that IntelliProfiler facilitates the identification of previously unknown signatures and group dynamics, contributing valuable insights to the field of behavioral neuroscience.

Introduction

Behavioral analyses using model animals are crucial for understanding neural functions and pathological states. Due to its ease of handling and suitability for genetic manipulations, the laboratory mouse is widely used as a model animal to study neural bases of various conditions, including psychiatric, neurodevelopmental, and neurodegenerative disorders. Traditional methods for analyzing neural functions in mice involve assessing behaviors, such as locomotion, exploration, social interaction, and learning/memory, through specific tests, including the open field test, the elevated plus maze, the social interaction test, and the Morris water maze[1–4]. However, these traditional approaches come with several limitations.

A major limitation of traditional behavioral analyses is the low throughput of data acquisition, as most analyses are manually conducted over limited periods under artificial conditions. Typically, behavior is recorded for a single mouse in a specific experimental setup. For instance, the open field test measures general locomotor activity and anxiety-related behavior by placing a single mouse in an open arena and tracking its movements and time spent in different zones[1]. Similarly, the three-chamber social interaction test assesses sociability by comparing the time a mouse interacts with a novel mouse versus an empty chamber, offering insights into social preferences[5]. A more significant concern is that interactions between experimenters and animals often introduce biases that influence results[6–8]. Handling by experimenters can elevate heart rate, body temperature, spontaneous activity, and anxiety, potentially impacting memory and learning abilities[7,9]. Moreover, variations in behavioral data have been linked to the researcher's gender and environmental conditions[8,10]. Therefore, there is a growing need for automated, unbiased systems to analyze behavior in natural (home-caged) conditions to ensure more robust and reliable data.

Recent advances in behavioral analyses have increasingly focused on studying group dynamics in semi-natural environments. One widely adopted approach is the use of radio frequency identification (RFID) technology, which enables the tracking of multiple animals within a home-cage setting. Compared to manual video tracking, RFID systems offer continuous, high-throughput data acquisition with minimal human intervention. IntelliCage, a pioneering RFID-based system, utilizes RFID readers placed at the corners of a cage to automatically monitor the frequency and timing of animals entering chambers[11]. IntelliCage has been widely used to investigate spontaneous behavior and learning in group-housed mice[12,13]. Another RFID-based system, ECO-HAB, consists of four open fields connected by tubes, with RFID readers positioned at

the junctions, allowing the study of free movement and social interactions among mice by tracking their movement between fields[14,15]. In addition, floor plate RFID systems have been developed to measure the locomotor activity of multiple animals simultaneously[16]. The first such system, "Trafficage", was introduced in 2005 by NewBehavior and later commercialized by TSE Systems[17–19], which was followed by "MultimouseMonitor", being brought to market by PhenoSys[20]. More recently, a high-resolution RFID floor plate system was developed by Dr. Toshihiro Endo and his team and has been commercialized by Phenovance (Japan), enabling the precise tracking of multiple animals with improved temporal resolution[21].

In this study, we developed IntelliProfiler, a software pipeline designed to analyze locomotor activity and social proximity using the above-mentioned commercially available RFID floor system. IntelliProfiler accommodates groups ranging from four to 16 mice while offering high spatial and temporal resolution. It enables long-term, continuous monitoring of activity and sociability with minimal researcher intervention. Using IntelliProfiler, we conducted 72-hour continuous behavioral analyses on large groups of male and female wild-type mice and compared behavioral patterns between sexes across age groups to investigate the effects of aging on social dynamics. Furthermore, we examined behavioral abnormalities in a model of autism spectrum disorder (ASD), focusing on offspring derived from aged fathers[22,23], to assess the impacts on social behavior. Collectively, our findings demonstrate that IntelliProfiler provides a powerful and efficient tool for investigating complex social behaviors and group dynamics in rodent models.

Results

IntelliProfiler software

Recording schema and physical configuration are shown in Fig. 1a and 1b. Raw data from the RFID floor array, including time, antenna ID, and transponder ID, were exported from the antenna board (Fig. 1c), converted into spatial coordinates and downgraded in a per-second resolution (Fig. 1d). Further calculations, analyses, and figure visualization were conducted using the converted data generated in the data collection and preprocessing step (Supplementary Fig. 1). We applied IntelliProfiler software to continuous 72-hour behavioral analyses on 8-week old male and female mice with group sizes of four, eight, and 16 mice (Fig. 1e). Due to the dislodging of one

RFID tag in the group of 16 male mice, data from 15 male mice were used for analysis, following the methodology of a previous article[24].

Locomotor activity

In the males, cumulative travel distances for every 2 hours exhibited the highest travel distance values in the four-mouse group than the eight- and 15-mouse groups during most of the time (Fig. 2a). The male mice exhibited the highest travel distance immediately after entry, dropping by less than half within 2 hours. Their travel distance increased again during the transition from light to dark period. In contrast, females showed less active and stable travel distances across almost all time points (Fig. 2b).

To understand the general trends of locomotor activity, we analyzed cumulative travel distances in 12-hour intervals. The males showed the highest travel distance just after their entry and significantly higher travel distance in the group of four mice than in the groups of eight and 15 mice (Fig. 2c). Small but significant differences were observed between the eight- and 15-mouse groups in the light period on day 1 and the dark period on day 3. On the other hand, females showed similar travel distances through the period among groups except for day 1 (Fig. 2d).

We then compared 2-hour intervals activities to examine sex differences. In the four-mouse group, male mice showed higher travel distances throughout the period than females, with significantly higher travel distances observed at six time points in the dark periods (Fig. 2e). However, no periodic trend was observed in eight- and 15/16-mouse groups (Fig. 2f, g). In the12-hour intervals (Fig. 2h-j), males showed higher travel distances throughout the period in the four-mouse group than female mice except for the light period on day 3 (Fig. 2h). On the other hand, no noticeable sex difference was observed in the groups of eight and 15/16 mice (Fig. 2i, j).

The time course of relative locomotor activity for each mouse was visualized as a heatmap. Male mice showed a marked increase in activity immediately after the introduction and at the onset of the dark period (Fig. 2k). A pronounced contrast of locomotor activity was observed between light and dark periods over 3 days (Fig. 2m). In contrast, female mice displayed relatively more variable activity patterns over time (Fig. 2l), with some showing elevated activity even during the light period (Fig. 2n). These findings suggest that male mice, particularly in smaller group sizes, exhibit

higher locomotor activity, pointing to potential sex-specific behavioral responses to group size.

Social interactions

To assess social interactions among group-housed mice, we tracked changes in the distance between two individual mice. The spatial relationships were classified into four categories based on proximities: "Same" - the other mouse occupied the same grid as the focal mouse; "Close" - the other mouse was in the adjacent grids; "Intermediate" - the other mouse was located beyond the surrounding grids; and "Away" (Fig. 3a). The transition in social distance ratios were recorded in 2-hour intervals for groups of four, eight, and 15 male mice and groups of four, eight, and 16 female mice.

The proportion of "Same" increased during the light period and decreased during the dark period in the four-mouse group, but this pattern was not observed in the other groups (Fig. 3b-g). A similar trend was found for the "Close," where its proportion rose in the light period and declined in the dark period across groups of four, eight, and 15 males and four, eight, and 16 females (Fig. 3b-g). The proportion of "Intermediate" was relatively low in the four-mouse group but increased with group size without showing a consistent periodic trend observed. In contrast, the proportion of "Away" decreased during the light period and increased in the dark period across all groups.

The average proportion of each social distance category during the light and dark periods was compared across groups. The proportion of "Same" decreased as group size increased. During the light period, the percentage of "Close" was higher than during the dark period across all groups, though there was no clear trend concerning group size. The proportion of "Intermediate" increased with group size during the light period and was higher in the eight- and 15/16-mouse groups than the four-mouse group during the dark period, but similar between the eight-mouse and 15/16-mouse groups. In contrast, the proportion of "Away" was highest in the 15-male group during both periods, although no clear pattern emerged for the female groups. These analyses revealed qualitatively distinct patterns of social distance in the eight- and 15/16-mouse groups compared to the four-mouse group.

Significant differences in the proportions of each category between the light and dark periods were observed in the groups of four males and four, eight, and 16 females (Fig. 3b, e-g). However, no significant differences were found in the eight and 15 male

groups (Fig. 3c, d). Regarding group size, significant differences were noted in the male groups during both the light and dark periods and in the female groups during the light period, but no significant differences were observed in the female groups during the dark period.

We then introduced the Close Contact Ratio (CCR), a metric to quantify social proximity to analyze social interactions. This ratio reflects the proportion of time two mice are either in the "Same" or "Close" (Fig. 4a). When CCR data were divided into 2-hour intervals for both male and female groups, males in the four-mouse group exhibited the highest CCR compared to the eight- and 15-mouse groups throughout the entire period. In male mice, the CCR was initially low immediately after entry, gradually increasing until 18:00, followed by a gradual decline until 20:00, with a similar pattern recurring from day 2 onward (Fig. 4b). In contrast, the females in the 16-mouse group showed a significantly lower CCR compared to the four- and eight-mouse groups (Fig. 4c), although no consistent time-dependent pattern was observed. We also analyzed the average CCR over 12-hour intervals. In male mice, the CCR decreased as the group size increased from four to eight to 15 mice during the light period (Fig. 4d). The 15-mouse group had the lowest CCR, while no significant difference was found between the four- and eight-mouse groups during the dark period. Similarly, female mice in the 16-mouse group tended to have the lowest CCR during the light period compared to the four- and eight-mouse groups, though no consistent differences were observed between the latter two groups (Fig. 4e). No clear trend was observed during the dark period in female mice.

We also examined the sex differences in CCR using 2-hour intervals in four-, eight-, and 15/16-mouse groups. In the four-mouse group, females showed a significantly higher CCR during the initial 4 hours (Fig. 4f). However, CCR fluctuated between males and females throughout the remaining time points, suggesting that consistent sex differences in social proximity might not be present in this group. In contrast, in the eight- and 15/16-mouse groups, females consistently exhibited higher CCR than males at most time points, indicating more pronounced sex differences in social proximity (Fig. 4g, h). To assess the overall trend, we analyzed the CCR in 12-hour intervals. In the four-mouse group, no clear sex differences in CCR were observed, except during the light period on day 2, when females had a higher CCR (Fig. 4i). However, in the eight-mouse group, females had a higher CCR than males across most periods, except during the dark period on day 3 (Fig. 4j). Similarly, in the 16-mouse group, females consistently exhibited a higher CCR than males across all the periods (Fig. 4k).

The time course of CCR, visualized as a heatmap for individual mice, revealed a strong periodic trend in the males, with CCRs peaking during the light period and decreasing during the dark period (Fig. 4l). In contrast, the female groups generally displayed higher CCRs for longer durations compared to males (Fig. 4l, m). The periodic patterns of CCRs were less pronounced in the 15/16 mouse groups, though the trend remained more apparent in males than females (Fig. 4l-o). These findings suggest that sex-specific social dynamics become more prominent in larger groups.

Aging effect

Since aging has been reported to affect many behavioral aspects, including locomotor activity and social interaction[25,26], we compared young (8-week-old) and aged (53-week-old) male mice in groups of four and eight (Fig. 1e and Supplementary Fig. 2-4). Aged males in the four-mouse group showed reduced social proximity, while those in the eight-mouse group exhibited prolonged movement durations, indicating that aging impacts activity and social behavior, particularly with group size.

Application into ASD model mice

We further applied IntelliProfiler to analyze behavior in a mouse model of ASD induced by advanced parental aging[27], using 8-week-old male and female offspring from young (YFO) or aged (AFO) fathers[22,23], housed in groups of eight or 16 (Fig. 1e).

In both group sizes, AFO males showed consistently increased travel distances across nearly all time points, while AFO females showed elevated activity at two-thirds of the time points (Fig. 5a-f). These effects were more pronounced in the 16-mouse group, with AFO males exhibiting greater cumulative distances, especially on Day 2 and during the light phase (Fig. 5g-l). Heatmaps indicate peak activity after cage introduction and at the onset of the dark phase, with AFO males displaying prolonged activity over time (Fig. 5m–t), suggesting altered temporal patterns.

Spatial proximity analysis revealed that AFO mice spent less time in close proximity and more time in intermediate or distant positions compared to YFO mice (Fig. 6a–i). CCR values were lower in AFO mice, especially in males during the dark phase and in females across both phases, with effects amplified in larger groups (Fig. 7a–g). AFO females showed higher CCRs values than males during the light phase (Fig. 7d, g, m), while cumulative CCRs confirmed reduced social proximity in AFO mice (Fig. 7h–l).

CCR heatmaps further revealed greater individual variability within the AFO groups (Fig. 7n–u).

Characterization of group behaviors

To investigate the behavioral characteristics of each group, we conducted principal component analysis (PCA) using four key parameters. First, we defined normalized activity as the activity at time *t*, divided by the maximum activity value recorded over Days 1-3, and multiplied by 100 to standardize the data. This allowed us to calculate the normalized activity in the light (AL) and dark (AD) periods by averaging activity values at each time point over three days. We selected four parameters for PCA: sociability, measured as CCR values during the light (SL) and dark (SD) periods (parameters 1 and 2, respectively), and normalized activity during the light (AL) and dark (AD) periods (parameters 3 and 4, respectively). The PCA results with estimated clusters are displayed in Fig. 8. Correlations among these parameters are shown in Supplementary Fig. 5-7. The number of clusters was determined using the Elbow method[27] and further assessed through Silhouette plots[28] (Supplementary Fig. 8-10).

The PCA revealed that the male mice in the 15-mouse group formed a well-defined separated cluster whereas the male and female mice in the four-mouse groups and female mice in the eight-mouse group clustered together (Fig. 8a). Female mice in the 16-mouse group split into two clusters, with one cluster aligning with the male mice in the eight-mouse group (Fig. 8b). In the feature space, AL and AD vectors pointed in the same direction, indicating similar patterns of activity, while SL and SD vectors diverged, reflecting different sociability dynamics between light and dark periods (Fig. 8c). In terms of aging effects, young and aged mice in the four-mouse groups were largely distributed, whereas those in the eight-mouse groups clustered near the origin (0,0) or in the negative X direction (Supplementary Fig. 9a). K-means clustering separated the four- and eight-mouse groups, indicating that aging influenced both activity and sociability in distinct ways (Supplementary Fig. 9b, c).

In the PCA analysis comparing AFO and YFO mice (Fig. 8d–f), AFO mice were primarily distributed along the negative axis of PC1, while YFO mice shifted toward the positive side. YFO females predominantly clustered in cluster 1, whereas AFO females were classified into clusters 2 or 3, indicating a clear group separation (Fig. 8e). In the feature space, AL and AD vectors aligned, while SL and SD diverged (Fig. 8f), highlighting distinct contributions of locomotor and social features.

Network analysis of social interactions

We explored how group size influences social interaction networks (Fig. 9). Qualitatively, there was no noticeable difference in network structure between male and female mice in the four- and eight-mouse groups (Fig. 9). However, in the 15/16-mouse groups, male mice exhibited increased social proximity and developed more expanded networks, influenced by light-dark circadian rhythms. In contrast, female mice maintained relatively uniform network structures (Fig. 9). When comparing young and aged male mice in the four-mouse groups, no significant differences in network structure were observed (Supplementary Fig. 11). In the eight-mouse groups, however, young male mice displayed increased social proximity and formed diverse networks that fluctuated with light-dark cycles, while aged male mice maintained more stable, uniform networks with only slight variation corresponding to circadian rhythms (Supplementary Fig. 11). When comparing YFO and AFO mice in both the eight- and 16-mouse groups, the social network structures of AFO males and females appeared more expanded than those of their YFO counterparts, with the more pronounced alterations observed in AFO female groups during the dark phase (Fig. 10). These findings suggest that male and female mice create distinct social environments and that aging may impact the complexity and heterogeneity of the networks in larger groups.

Analysis of individual social interactions

Lastly, we focused on individual differences in social interactions through a pairwise analysis of CCR. No obvious individual differences were observed between sexes in the four- and eight-mouse groups (Supplementary Fig. 12-14). However, in the 15/16-mouse groups, two males (mouse ID #1 and #2) exhibited lower CCR scores than the others. Regarding the aging effect, aged males showed lower CCR scores and more ambiguous, less defined time-dependent patterns than young males (Supplementary Fig. 15-17). These findings suggest that individuality may develop progressively with aging in males, potentially contributing to the observed social dynamics.

Discussion

298 In this study, we implemented “IntelliProfiler,” a software pipeline developed to process
299 raw positional data collected via a commercially available RFID floor plate system. The
300 antenna board used in our study has previously been described as “a high-resolution
301 RFID floor plate” in a recent review paper on IntelliCage system[21]. By applying
302 IntelliProfiler, we gained novel insights into how group size, sex, and aging influence
303 on locomotor activity and social proximity, thereby providing a more comprehensive
304 understanding of semi-natural behaviors in group-housed mice.

305 One of our key findings was the impact of group size on behavior. IntelliProfiler
306 revealed significant differences in activity levels and social proximity. Traditional
307 behavior paradigms are typically designed for individual animals[29,30] and might fail to
308 capture the complexities of behavior in groups. A recent article emphasized the
309 importance of studying animals under 'natural conditions'[31]. IntelliProfiler enables us to
310 monitor authentic locomotor activity under semi-natural conditions, offering a more
311 comprehensive understanding of how group size shapes individual activity and social
312 dynamics.

313 We introduced CCR as a novel social parameter to measure social proximity,
314 representing a significant advancement in behavioral analysis (Fig. 4). Traditional social
315 interaction tests offer limited insight into short-term interactions, but the CCR provides
316 a more detailed, long-term view of group dynamics. We found that females tended to
317 form stable clusters, while males exhibited more fluid, group size-dependent social
318 patterns (Fig. 4, 8, 9). This underscores IntelliProfiler’s ability to detect subtle yet
319 important sex-specific social behaviors, often overlooked by conventional methods.

320 Previous studies using depth-sensing or RFID-assisted video tracking systems have
321 enabled detailed assessment of social behaviors such as approaching, avoiding, or
322 attacking by detecting animal orientation with the high spatial resolution[32–35]. However,
323 these systems are typically limited in the number of animals that can be tracked
324 simultaneously. In contrast, the CCR metric used in our study reflects spatial proximity
325 but does not directly capture specific social actions. Still, time-resolved CCR
326 trajectories may support broader analyses of such social interactions. Notably, CCR
327 analysis avoids identity-swapping errors that can occur in video tracking with large
328 groups.

329 Aging affected both locomotor activity and social interactions, with aged males
330 showing more variable and less distinct CCR patterns compared to young males
331 (Supplementary Fig. 3-4). In the eight-mouse group, aged males exhibited higher

activity levels than younger males (Supplementary Fig. 2), contrasting with studies using open field test that reported reduced or similar travel distances in aged mice[26,36]. This discrepancy likely stems from differences in the experimental context—short-term, single-animal testing in a novel environment versus long-term monitoring in group-housed, semi-natural settings. In terms of social behavior, our findings align with previous reports of reduced contact frequency and shorter interaction durations in aged mice[26].

To assess behavioral variability, we analyzed coefficient of variation (CV) for both travel distance and CCR across experimental conditions (Supplementary Fig. 20-23). CVs for travel distance increased with group size in both sexes (Supplementary Fig. 20e–f), while aged males showed similar variability to young males in smaller groups (Supplementary Fig. 20g–l), suggesting that aging had limited impact on variability. A similar trend was observed for CCR: male mice showed greater variability with increasing group sizes, whereas females maintained more consistent (Supplementary Fig. 22e–f). AFO mice showed lower variability in travel distance compared to YFO mice (Supplementary Fig. 21), although both groups exhibited increased CCR variability with larger group sizes (Supplementary Fig. 23). These results suggest that behavioral variability is shaped by group size and sex, and epigenetic factors such as advanced paternal age. Elevated CVs in large male groups may reflect greater heterogeneity or emerging social stratification. A limitation of this study is that the AFO and YFO mice were housed and recorded in different facilities, which may have introduced confounding effects.

Our findings show that AFO mice, a model of ASD, exhibited increased locomotor activity and reduced social proximity compared to YFO mice, particularly in larger groups (Fig. 5–7). While previous studies reported no difference[37] or reduced activity in AFO mice[38], our group-housed analysis revealed increased locomotor activity, suggesting a context-dependent phenotype that emerges only under ecologically valid conditions. Regarding social behavior, prior studies have shown reduced sociability in AFO mice, especially with advanced paternal age[37–39]. Consistent with these reports, IntelliProfiler detected lower CCR values in AFO mice, particularly in larger groups─a pattern not observed in our previous study[40]. These results underscore the utility of IntelliProfiler as a context-sensitive platform for detecting subtle behavioral phenotypes in neurodevelopmental disorder models.

The special resolution of IntelliProfiler is limited by the 5 x 5 cm grid size of the antenna board. The resolution is sufficient for proximity-based analyses, such as

huddling or sleeping, where each grid typically contains only a few mice. However, higher resolution may be needed to capture fine-scale interactions like mating or grooming. Notably, one RFID tag detached from a male mouse in the 16-mouse group, resulting in no movement data from Day 2 onward. As the untagged mouse remained in the cage, this may have slightly biased the social interaction data.

Despite its advantages, IntelliProfiler has a few limitations. First, its spatial resolution is lower than video-based tracking systems like DLC[41,42], as the current grid size is 5 cm x 5 cm, allowing two mice located in parallel. Determining body orientation is also challenging when the animal remains within the same grid. Second, the system has difficulty distinguishing detailed social contacts, such as sniffing, mounting, or huddling. Lastly, the current RFID system requires surgery for transponder implantation, and it is not yet possible to eliminate the invasive effects due to the size of commercially available transponders. These challenges should be addressed in future developments.

It has been reported that invasive interventions, such as intracranial surgery, can reduce continuous locomotor activity[43]. Although the RFID-tag implantation is considerably less invasive than neurosurgical procedures, we allowed a one-week recovery prior to behavioral assessments, following a previous study that implemented subcutaneous RFID transponder implantation in the abdominal region[44]. Another study reported that mice in pain may be social avoided by conspecifics under naturalistic conditions, suggesting that healthy animals might actively avoid individuals experiencing disconfort[45]. In our experimental design, such avoidance responses were likely minimized, as all mice underwent RFID tag implantation, thereby standardized the physical condition and procedural experience across the group.

IntelliProfiler offers significant advantages in scalability and adaptability for high-throughput behavioral experiments in semi-naturalistic settings. This is especially valuable for neuroscience research, where subtle behavioral differences are often critical. By enabling long-term, large-scale data collection with minimal human intervention, IntelliProfiler reduces experimenter bias and improves reproducibility.

The CCR metric provides a standardized, scalable measure of social interaction, positioning IntelliProfiler as a versatile platform for behavioral phenotyping. Its broad utility spans from basic neuroscience to translational preclinical research, with strong potential to advance studies on social behavior, neurodevelopmental disorders, and future pharmacological interventions.

IntelliProfiler may also be applied to other rodent model species, such as rats, degus, and guinea pigs, which exhibit pronounced social or nurturing behaviors[46–48]. Additionally, the system could support quantitative assessment in models of neurodegenerative diseases, like Alzheimer's, by capturing spontaneous activity patterns─offering a potential alternative to conventional behavioral testing protocol[49,50].

Conclusion

IntelliProfiler offers a significant advancement in animal behavior research by enabling continuous, detailed, and unbiased analysis of individual movements and social interactions within dynamic and complex group environments. In this study, we demonstrated its utility in uncovering the critical influence of group size, sex, aging, and an ASD model on behavioral patterns. As a robust and versatile platform, IntelliProfiler facilitates the study of behavior in more naturalistic settings, opening new avenues for large-scale behavioral research and provide deeper insights into social dynamics.

Methods

Animals

C57BL/6J mice at 7- or 52-week old were purchased from CLEA Japan, Inc., and maintained in the animal facility at Tohoku University Graduate School of Medicine. To generate aged father-derived offspring (AFO) at 7-week old, 54–60-week-old male mice were mated with 8–12-week-old female mice. The mice were recovered for 1 week before starting behavioral recording. The recordings started at 8- or 53-week old. All experimental procedures were approved by the Ethics Committee for Animal Experiments at the Tohoku University Graduate School of Medicine (approval number: 2021MdA-020-13).

RFID implementation

An RFID tag (7 mm × 1.25 mm, Phenovance, Japan) was subcutaneously implanted into the abdominal region of each mouse under anesthesia. The surgical protocol was described in detail in the Supplementary Information.

Hardware

The antenaboard has been developed by Dr. Endo and his colleagues and is commercially available (eeeHive 2D, Phenovance LCC, Japan)[21]. The antenaboard consists of 96 antenna tiles (5 cm by 5 cm each) arranged in 12x8 grids (Fig. 1a). The home cage was 2000P cage (58 cm x 38 cm x 21.5 cm = width × depth × height, Tecniplast, Italy), equipped with a cage lid with food pellets, and three water bottles for long-term housing (Fig. 1a, b). The antenaboard and home cage were placed inside a soundproof box (Phenovance LCC, Japan). The light-dark cycle in the soundproof box and testing room was 12:12 hours (08:00-20:00, light; 20:00-08:00, dark). Mice were introduced at 8:00 in the light period on day 1.

Software

R language (Version 4.2.2) was mainly used for preprocessing, data analysis, and visualization[51]. Python (Version 3.9.7), Prism 9, and Microsoft Excel (Version 16.86) were also used for preprocessing, data analysis, and visualization. R and Python packages required for the scripts are listed in Supplementary Table 1. All custom scripts are publicly available in a GitHub repository (see “Code Availability”).

Data Collection and Preprocessing

Data, including time, antenna ID, and transponder ID, were exported from the antenabord via Universal Serial Bus (USB) using TeraTerm software (Fig. 1c). The raw data were converted into a format per second with time, antenna ID, transponder ID, and X-Y coordinates (Fig. 1d). Missing values were interpolated by the immediately preceding value. These operations were implemented using a custom R script, 'IP_general.R'.

Flow Chart of IntelliProifler Pipeline:
The workflow is illustrated in Supplementary Fig. 1. Each stage: data collection, preprocessing and feature extraction, close contact ratio (CCR) computation, and advanced analysis is shown in Supplementary Information.

Data Availability
The behavioral data generated are provided in Supplementary Information and tables.

Code Availability
All code and scripts used for data analysis are available on GitHub.
- Repository URL: https://github.com/ShoheiOchi/IntelliProfiler

References

1. Hall, C. S. Emotional behavior in the rat. I. Defecation and urination as measures of individual differences in emotionality. *J Comp Psychol* **18**, 385–403 (1934).
2. Pellow, S., Chopin, P., File, S. E. & Briley, M. Validation of open:closed arm entries in an elevated plus-maze as a measure of anxiety in the rat. *J Neurosci Methods* **14**, 149–167 (1985).
3. File, S. E. & Hyde, J. R. Can social interaction be used to measure anxiety? *Br. J. Pharmac* **62**, 19–24 (1978).
4. Morris, R. Developments of a water-maze procedure for studying spatial learning in the rat. *J Neurosci Methods.* **11**, 47–60 (1984).
5. Moy, S. S. *et al.* Sociability and preference for social novelty in five inbred strains: an approach to assess autistic-like behavior in mice. *Genes Brain Behav* **3**, 287–302 (2004).
6. Balcombe, J. P., Barnard, N. D. & Sandusky, C. Laboratory routines cause animal stress. *Contemp Top Lab Anim Sci* **43**, 42–51 (2004).
7. Gouveia, K. & Hurst, J. L. Optimising reliability of mouse performance in behavioural testing: The major role of non-aversive handling. *Sci Rep* **7:44999**, (2017).
8. Georgiou, P. *et al.* Experimenters' sex modulates mouse behaviors and neural responses to ketamine via corticotropin releasing factor. *Nat Neurosci* **25**, 1191–1200 (2022).
9. Hurst, J. L. & West, R. S. Taming anxiety in laboratory mice. *Nat Methods* **7**, 825–826 (2010).
10. Sorge, R. E. *et al.* Olfactory exposure to males, including men, causes stress and related analgesia in rodents. *Nat Methods* **11**, 629–632 (2014).
11. Lipp, H.-P. High-throughput and automated behavioural screening of normal and genetically modified mice. *Business Briefing: Future Drug Discovery* 1–5 (2005).
12. Endo, T. *et al.* Automated test of behavioral flexibility in mice using a behavioral sequencing task in IntelliCage. *Behavioural Brain Research* **221**, 172–181 (2011).
13. Kiryk, A. *et al.* IntelliCage as a tool for measuring mouse behavior – 20 years perspective. *Behavioural Brain Research* **388**, (2020).
14. Chen, X. *et al.* Modelling collective behavior in groups of mice housed under semi-naturalistic conditions. *bioRxiv* (2024) doi:10.1101/2023.07.26.550619.

15. Winiarski, M. *et al.* Social deficits in BTBR T+ Itpr3tf/J mice vary with ecological validity of the test. *Genes Brain Behav* **21**, (2022).
16. Klein, C. J. M. I. *et al.* Measuring Locomotor Activity and Behavioral Aspects of Rodents Living in the Home-Cage. *Frontiers in Behavioral Neuroscience* vol. 16 Preprint at https://doi.org/10.3389/fnbeh.2022.877323 (2022).
17. Onishchenko, N. *et al.* Prenatal exposure to PFOS or PFOA alters motor function in mice in a sex-related manner. *Neurotox Res* **19**, 452–461 (2011).
18. Dudek, M. *et al.* A comparison of the anorectic effect and safety of the alpha2-adrenoceptor ligands guanfacine and yohimbine in rats with diet-induced obesity. *PLoS One* **10**, (2015).
19. Kotańska, M. *et al.* KSK19 – Novel histamine H3 receptor ligand reduces body weight in diet induced obese mice. *Biochem Pharmacol* **168**, 193–203 (2019).
20. Frahm, S. *et al.* Alpha-Synuclein transgenic mice, h-α-SynL62, display α-Syn aggregation and a dopaminergic phenotype reminiscent of Parkinson's disease. *Behavioural Brain Research* **339**, 153–168 (2018).
21. Lipp, H. P. *et al.* IntelliCage: the development and perspectives of a mouse- and user-friendly automated behavioral test system. *Front Behav Neurosci* **17**, (2024).
22. Mai, L. *et al.* Advanced paternal age diversifies individual trajectories of vocalization patterns in neonatal mice. *iScience* **25**, (2022).
23. Yoshizaki, K. *et al.* Paternal age affects offspring via an epigenetic mechanism involving REST/NRSF. *EMBO Rep* **22**, (2021).
24. Smutek, M. *et al.* A model of alcohol drinking under an intermittent access schedule using group-housed mice. *PLoS One* **9**, (2014).
25. Yanai, S. & Endo, S. Functional Aging in Male C57BL/6J Mice Across the Life-Span: A Systematic Behavioral Analysis of Motor, Emotional, and Memory Function to Define an Aging Phenotype. *Front Aging Neurosci* **13**, (2021).
26. Shoji, H., Takao, K., Hattori, S. & Miyakawa, T. Age-related changes in behavior in C57BL/6J mice from young adulthood to middle age. *Mol Brain* **9**, (2016).
27. Thorndike, R. L. Who belongs in the family? *Psychometrika* **18**, 267–276 (1953).
28. Rousseeuw, P. J. Silhouettes: A graphical aid to the interpretation and validation of cluster analysis. *J Comput Appl Math* **20**, 53–65 (1987).
29. Yoshizaki, K. *et al.* Paternal aging affects behavior in Pax6 mutant mice: A gene/environment interaction in understanding neurodevelopmental disorders. *PLoS One* **11**, (2016).

30. Crawley, J. N. Exploratory behavior models of anxiety in mice. *Neurosci Biobehav Rev* **9**, 37–44 (1985).
31. Smith, K. Lab mice go wild: making experiments more natural in order to decode the brain. *Nature* **618**, 448–450 (2023).
32. Peleh, T., Bai, X., Kas, M. J. H. & Hengerer, B. RFID-supported video tracking for automated analysis of social behaviour in groups of mice. *Journal of Neuroscience Methods* vol. 325 Preprint at https://doi.org/10.1016/j.jneumeth.2019.108323 (2019).
33. Sakamoto, N. *et al.* Marker-less tracking system for multiple mice using Mask R-CNN. *Front Behav Neurosci* **16**, (2023).
34. Segalin, C. *et al.* The Mouse Action Recognition System (MARS) software pipeline for automated analysis of social behaviors in mice. **10**, (2021).
35. Hong, W. *et al.* Automated measurement of mouse social behaviors using depth sensing, video tracking, and machine learning. *Proc Natl Acad Sci U S A* **112**, E5351–E5360 (2015).
36. Shoji, H. & Miyakawa, T. Age-related behavioral changes from young to old age in male mice of a C57BL/6J strain maintained under a genetic stability program. *Neuropsychopharmacol Rep* **39**, 100–118 (2019).
37. Tanaka, M. *et al.* Interaction between social behavior and paternal age in offspring of the same paternal mice. *Neuropsychopharmacol Rep* **42**, 343–346 (2022).
38. Zhao WL *et al.* Autism-like behaviors and abnormality of glucose metabolism in offspring derived from aging males with epigenetically modified sperm. *Aging (Albany NY)* 19766–19784 (2020).
39. Mao, Y. *et al.* Advanced paternal age exacerbates neuroinflammation in offspring via m6A modification-mediated intergenerational inheritance. *J Neuroinflammation* **21**, 249 (2024).
40. Yoshizaki, K. *et al.* Paternal age affects offspring's behavior possibly via an epigenetic mechanism recruiting a transcriptional repressor REST. Preprint at https://doi.org/10.1101/550095 (2019).
41. Lauer, J. *et al.* Multi-animal pose estimation, identification and tracking with DeepLabCut. *Nat Methods* **19**, 496–504 (2022).
42. Mathis, A. *et al.* DeepLabCut: markerless pose estimation of user-defined body parts with deep learning. *Nat Neurosci* **21**, 1281–1289 (2018).

43. Abdollahi Nejat, M., Stiedl, O., Smit, A. B. & van Kesteren, R. E. Continuous locomotor activity monitoring to assess animal welfare following intracranial surgery in mice. *Front Behav Neurosci* **18**, (2024).
44. Bains, R. S. *et al.* Assessing mouse behaviour throughout the light/dark cycle using automated in-cage analysis tools. *J Neurosci Methods* **300**, 37–47 (2018).
45. Le Moëne, O. & Larsson, M. Social Avoidance of Mice in Pain in Naturalistic Conditions. *Affect Sci* (2024) doi:10.1007/s42761-024-00276-8.
46. Von Engelhardt, N., Kowalski, G. J. & Guenther, A. The maternal social environment shapes offspring growth, physiology, and behavioural phenotype in guinea pigs. *Front Zool* **12**, (2015).
47. Nagy, M. *et al.* Long-term tracking of social structure in groups of rats. (2024) doi:10.1038/s41598-024-72437-5.
48. Rivera, D. S. *et al.* Effects of long-lasting social isolation and re-socialization on cognitive performance and brain activity: a longitudinal study in Octodon degus. *Sci Rep* **10**, (2020).
49. Codita, A. *et al.* Impaired behavior of female tg-ArcSwe APP mice in the IntelliCage: A longitudinal study. *Behavioural Brain Research* **215**, 83–94 (2010).
50. Winslow, W. *et al.* IntelliCage Automated Behavioral Phenotyping Reveals Behavior Deficits in the 3xTg-AD Mouse Model of Alzheimer's Disease Associated With Brain Weight. *Front Aging Neurosci* **13**, (2021).
51. R Core Team. R: A Language and Environment for Statistical Computing. R Foundation for Statistical Computing, Vienna. (2021).

Acknowledgements

The authors are grateful to Dr. Ken-ichiro Tsutsui for temporally providing the behavioral analysis environment, and Kentaro Abe for advising on the setup of the behavioral analysis room. We also thank Dr. Toshihiro Endo and his colleagues for developing a RFID floor array used in this study, especially, Dr. Endo for technical advices. This research was funded by the JSPS KAKENHI under grant number 24H01419 (to S.O.) and 24K02203 (to N.O.), AMED under grant number JP21wm0425003 (to N.O.) 24wm0225044h0001 (to S.O.). Takeda Science Foundation (to S.O.) and FY2024 Tohoku University Graduate School of Medicine Grant-in-Aid for Joint Research by Young Researchers (to S.O.).

Contributions

Conceptualization, S.O., H.I. and N.O.; behavior analysis, S.O.; data process, S.O. and H.I.; code preparation, S.O. and H.I.; figure preparation, S.O.; writing—review and editing, S.O., H.I. and N.O.; supervision, N.O.; project administration, S.O. and N.O.; funding acquisition, S.O., and N.O. All authors have read and agreed to the published version of the manuscript.

Figure Legends

Fig. 1: IntelliProfiler software automated behavioral measurement system.

a Schematic of RFID floor plate (Phenovace) and IntelliProfiler software. The system tracks the location of mice implanted with RFID tags via detectors placed in a 96-grid array at the base, with each grid measuring 5 cm x 5 cm. Location information is converted into XY coordinates (X=12, Y=8), based on antenna IDs (1-96). **b** Photograph of the IntelliProfiler. **c** Original data, capturing information on Time, Antenna ID, and Transponder ID. **d** Processed data converted for the IntelliProfiler. The data is refined to include Time, Antenna ID, Transponder ID, and XY coordinates. Decimal information is removed from the time data. If multiple individuals are detected on the same antenna ID simultaneously, their information is separated into different rows. **e** Behavior analysis was conducted over a continuous 72-hour period for male and female mice in groups of four-, eight- and 15/16. Young (8-week old) and aged (53-week old) male mice were analyzed in groups of four and eight. Young father derived offspring (YFO) and aged father derived offspring (AFO) male and female mice were analyzed in groups of eight and 16.

Fig. 2: Activity analysis of group-housed mice using the IntelliProfiler software.

a-j Cumulative travel distances measured in 2-hour intervals (**a, b, e-g**) and over 12-hour intervals (light-dark cycles) (**c, d, h-j**). **a-d** Analysis of locomotor activity based on group size, comparing groups of four, eight, and 15 males (**a, c**) and four, eight, and 16 female mice (**b, d**). **e-j** Analysis of sex differences in locomotor activity, comparing groups of four (**e, h**), eight (**f, i**) and 15-16 (**g, j**) male and female mice. **k-n** Heatmaps showing relative locomotor activity over 2-hour intervals (**k, l**) and 12-hour intervals (**m, n**) for groups of four, eight, and 15-16 mice. Values in the bar or line graphs are presented as mean ± SD, with box plots displaying min/max whiskers. Statistical analysis was conducted using Holm-Sidak method for multiple comparison. Significance levels are indicated as $*p < 0.05$, $**p < 0.01$, and $***p < 0.001$. $p < 0.001$ (**c**), $p = 0.011$ (**d**), $p < 0.001$ (**e**), $p = 0.894$ (**f**), $p = 0.009$ (**g**), $p < 0.001$ (**h**), $p = 0.920$ (**i**), $p = 0.139$ (**j**).

Fig. 3: The spatial relationships among group-housed mice using the IntelliProfiler software.

a Definition of the spatial relationships between two individual mice. When another mouse is in the same grid as the focal mouse (both depicted in yellow), the relationship is defined as "Same." If the other mouse is in the surrounding grids (depicted in olive),

654 it is defined as “Close.” If the other mouse is outside the surrounding grids (depicted in
655 indigo), it is defined as “Intermediate.” If the other mouse is beyond the “Intermediate”
656 zone (depicted in blue), the relationship is categorized as “Away.” **b-g** The 2-hour bin
657 transition of proportions based on “Same,” “Close,” “Intermediate,” and “Away” for
658 groups of four male mice (**b**), eight male mice (**c**), 15 male mice (**d**), four female mice
659 (**e**), eight female mice (**f**), and 16 female mice (**g**). The average proportion of distance
660 categories during the light period and the dark period is shown for each group. Chi-
661 square *p*-values comparing the proportions between light and dark periods: $p < 0.001$ (**b**,
662 four males), $p = 0.256$ (**c**, eight males), $p = 0.114$ (**d**, 15 males), $p = 0.005$ (**e**, four
663 females), $p = 0.049$ (**f,** eight females), $p = 0.007$ (**g**, 16 females). The *p*-values of chi-
664 square for the group size, $p < 0.001$ (**b-d**, males in the light phase), $p = 0.002$ (**b-d**,
665 males in the dark phase), $p < 0.001$ (**e-g**, females in the light phase), $p = 0.092$ (**e-g**,
666 females in the dark phase).
667
668 **Fig. 4: Close contact between two individuals among group-housed mice analyzed**
669 **using the IntelliProfiler software.**
670 **a** Definition of close contact, where two mice either in the “Same” grid (depicted in
671 yellow) or in adjacent grids, classified as “Close” (depicted in olive). **b-k** Average
672 Close Contact Ratio (CCR) measured in in 2-hour intervals (**b, c, f-h**) and 12-hour
673 intervals (**d, e, i-k**). **b-e** Analysis of CCR based on group size, comparing groups of
674 four, eight, and 15 male mice (**b, d**) and four, eight, and 16 female mice (**c, e**). **f-k**
675 Analysis of sex differences in CCR, comparing groups of four (**f, i**), eight (**g, j**) and
676 15/16 (**h, k**) male and female mice. **l-o** Heatmaps showing the time course of CCR over
677 2-hour intervals (**l, m**) and 12-hour intervals (**n, o**) for groups of four, eight, and 15-16
678 mice. Values in the bar or line graphs are presented as mean ± SD, with box plots
679 showing min/max whiskers. Statistical analysis was conducted using Holm-Sidak
680 method for multiple comparisons. Significance levels are indicated as $*p < 0.05$, $**p <$
681 0.01, and $***p < 0.001$. $p < 0.001$ (**b**), $p < 0.001$ (**c**), $p = 0.882$ (**f**), $p < 0.001$ (**g**), $p <$
682 0.001 (**h**), $p = 0.873$ (**i**), $p < 0.001$ (**j**), $p < 0.001$ (**k**).
683
684 **Fig. 5: Activity analysis of group-housed male and female aged father derived**
685 **offspring (AFO) mice using the IntelliProfiler software.**
686 **a-f** Cumulative travel distances measured in 2-hour intervals for 2 days (**a-c**) and for 3
687 days (**d-f**) and over 12-hour intervals for 2 days (**g-i**) and for 3 days (**j-l**). **a-l** Analysis of
688 locomotor activity based on group size, comparing groups of eight and 15/16 young
689 father derived offspring (YFO) and aged father derived offspring (AFO) mice. **a-l**

690 Analysis of parental aging effects in locomotor activity, comparing groups of eight and
691 15/16 male YFO and AFO mice (**a, d, g, j**), groups of eight and 16 female YFO and
692 AFO mice (**b, e, h, k**), groups of eight and 16 male and female AFO mice (**c, f, i, l**). **m-t**
693 Heatmaps showing relative locomotor activity over 2-hour intervals (**m, n, q, r**) and 12-
694 hour intervals (**o, p, s, t**) for groups of eight and 16 mice. Values in the bar or line
695 graphs are presented as mean ± SD, with box plots displaying min/max whiskers.
696 Statistical analysis was conducted using Holm-Sidak method for multiple comparisons.
697 Significance levels are indicated as $*p < 0.05$, $**p < 0.01$, and $***p < 0.001$.
698
699 **Fig. 6: The spatial relationships among group-housed male and female AFO mice**
700 **using the IntelliProfiler software.**
701 **a** Definition of the spatial relationships between two individual mice. When another
702 mouse is in the same grid as the focal mouse (both depicted in yellow
703), the relationship is defined as "Same." If the other mouse is in the surrounding grids
704 (depicted in olive), it is defined as "Close." If the other mouse is outside the
705 surrounding grids (depicted in indigo), it is defined as "Intermediate." If the other
706 mouse is beyond the "Intermediate" zone (depicted in blue), the relationship is
707 categorized as "Away." **b-e** The 2-hour bin transition of proportions based on "Same,"
708 "Close," "Intermediate," and "Away" for groups of eight male YFO mice (**b**), eight
709 female YFO mice (**c**), eight male AFO mice (**d**), eight female AFO mice (**e**), 15 male
710 YFO mice (**f**), 16 female YFO mice (**g**), 16 male AFO mice (**h**), 16 female AFO mice
711 (**i**). **b-i** The average proportion of distance categories during the light period and the
712 dark period is shown for each group. Chi-square *p*-values comparing the proportions
713 between light and dark periods, $p = 0.359$ (**b**, eight male YFO), $p = 0.215$ (**c**, eight
714 female YFO), $p < 0.001$ (**d**, eight male AFO), $p < 0.001$ (**e**, eight female AFO), $p =$
715 0.114 (**f**, 15 male YFO), $p = 0.007$ (**g**, 16 female YFO), $p = 0.050$ (**h**, 16 male AFO), p
716 < 0.001 (**i**, 16 female AFO).
717
718 **Fig. 7: Close contact between two individuals among group-housed male and**
719 **female AFO mice analyzed using the IntelliProfiler software.**
720 **a** Definition of close contact, where two mice either in either "Same" (depicted in
721 yellow) or in adjacent grids, classified as "Close" (depicted in olive). **b-h** Average
722 Close Contact Ratio (CCR) measured in 2-hour intervals (**b-g**) and 12-hour intervals (**h-**
723 **m**). **b, e, h, k** Analysis of CCR based on group size, comparing groups of eight and
724 15/16 male YFO and AFO. **c, f, i, l** Analysis of CCR based on group size, comparing
725 groups of eight and 16 female YFO and AFO. **d, g, j, m** Analysis of CCR based on

group size, comparing groups of eight and 16 male AFO and female AFO. **n-u** Heatmaps showing the time course of CCR over 2-hour intervals (**n, o, r, s**) and 12-hour intervals (**p, q, t, u**) for groups of eight and 15/16 mice. Values in the bar or line graphs are presented as mean ± SD, with box plot showing min/max whiskers. Statistical analysis was conducted using Holm-Sidak method for multiple comparisons. Significance levels are indicated as $*p < 0.05$, $**p < 0.01$, and $***p < 0.001$. $p < 0.001$ (**c**), $p = 0.338$ (**d**), $p = 0.072$ (**e**), $p < 0.001$ (**f**), $p = 0.007$ (**g**), $p = 0.109$ (**h**).

Fig. 8: Principal component analysis of group behavior using the IntelliProfiler software.

a-f Principal component analysis (PCA) of group behavior in four, eight, and 15/16 male and female mice (**a-c**) and in AFO and YFO mice in groups of eight and 15/16 (**d-f**). **b, e** K-means clustering in PCA plots. **c, f** Analysis of feature vectors, focusing on Close Contact Ratio (CCR) and relative activity during the light and dark periods.

Fig. 9: Network analysis of social interaction in the male and female mice using the IntelliProfiler software.

Network analysis of social interactions during the light period on day 1 and the dark period on day 3 in groups of four, eight, and 15/16 male and female mice. Nodes represents individual mice, and edges reflects the relative social contacts between two individuals. The network graph was generated using Cytoscape. **Supplementary Fig. 12** provides additional network diagrams, where unique color code for each individual highlighted the individual-specific social dynamics within the network.

Fig. 10: Network analysis of group interaction in male and female AFO mice using the IntelliProfiler software.

Network analysis of social interactions during the light period on day 1 and the dark period on day 3 in groups of four and eight and 15/16 male and female YFO and AFO mice. Each circle represents an individual mouse, and the proximity of the lines indicates the relative social distance between two individuals. The network graph was generated using Cytoscape.

Fig. 1.

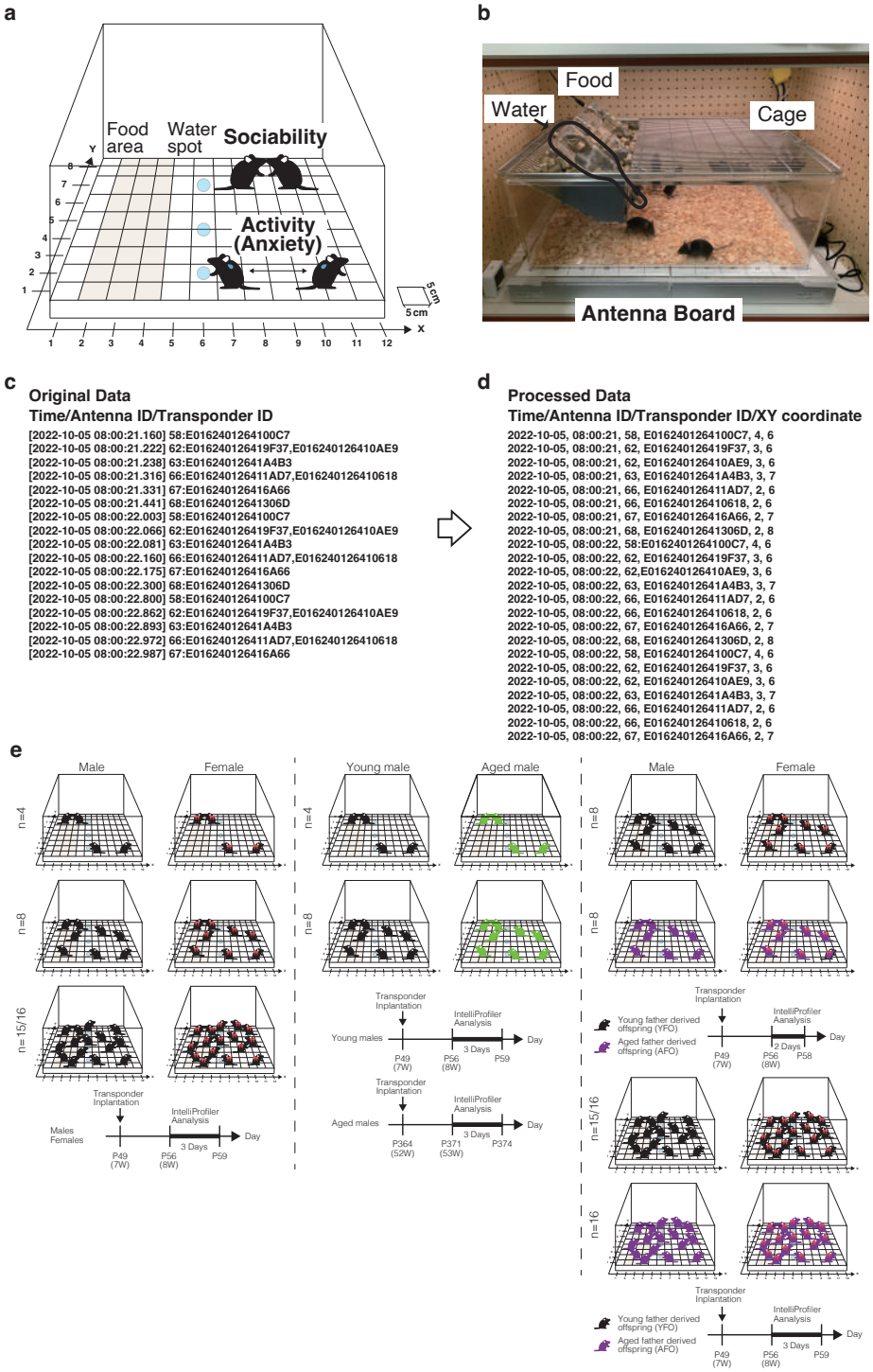
a
Food area
Water spot
Sociability
Activity (Anxiety)
Y
X
5 cm
5 cm
b
Food
Water
Cage
Antenna Board
c
Original Data
Time/Antenna ID/Transponder ID
[2022-10-05 08:00:21.160] 58:E0162401264100C7
[2022-10-05 08:00:21.222] 62:E016240126419F37,E016240126410AE9
[2022-10-05 08:00:21.238] 63:E01624012641A4B3
[2022-10-05 08:00:21.316] 66:E01624012641AD7,E016240126410618
[2022-10-05 08:00:21.331] 67:E016240126416A66
[2022-10-05 08:00:21.441] 68:E01624012641306D
[2022-10-05 08:00:22.003] 58:E0162401264100C7
[2022-10-05 08:00:22.066] 62:E016240126419F37,E016240126410AE9
[2022-10-05 08:00:22.081] 63:E01624012641A4B3
[2022-10-05 08:00:22.160] 66:E01624012641AD7,E016240126410618
[2022-10-05 08:00:22.175] 67:E016240126416A66
[2022-10-05 08:00:22.300] 68:E01624012641306D
[2022-10-05 08:00:22.800] 58:E0162401264100C7
[2022-10-05 08:00:22.862] 62:E016240126419F37,E016240126410AE9
[2022-10-05 08:00:22.893] 63:E01624012641A4B3
[2022-10-05 08:00:22.972] 66:E01624012641AD7,E016240126410618
[2022-10-05 08:00:22.987] 67:E016240126416A66
d
Processed Data
Time/Antenna ID/Transponder ID/XY coordinate
2022-10-05, 08:00:21, 58, E0162401264100C7, 4, 6
2022-10-05, 08:00:21, 62, E016240126419F37, 3, 6
2022-10-05, 08:00:21, 62, E016240126410AE9, 3, 6
2022-10-05, 08:00:21, 63, E01624012641A4B3, 3, 7
2022-10-05, 08:00:21, 66, E01624012641AD7, 2, 6
2022-10-05, 08:00:21, 66, E016240126410618, 2, 6
2022-10-05, 08:00:21, 67, E016240126416A66, 2, 7
2022-10-05, 08:00:21, 68, E01624012641306D, 2, 8
2022-10-05, 08:00:22, 58:E0162401264100C7, 4, 6
2022-10-05, 08:00:22, 62, E016240126419F37, 3, 6
2022-10-05, 08:00:22, 62,E016240126410AE9, 3, 6
2022-10-05, 08:00:22, 63, E01624012641A4B3, 3, 7
2022-10-05, 08:00:22, 66, E01624012641AD7, 2, 6
2022-10-05, 08:00:22, 66, E016240126410618, 2, 6
2022-10-05, 08:00:22, 67, E016240126416A66, 2, 7
2022-10-05, 08:00:22, 68, E01624012641306D, 2, 8
2022-10-05, 08:00:22, 58, E0162401264100C7, 4, 6
2022-10-05, 08:00:22, 62, E016240126419F37, 3, 6
2022-10-05, 08:00:22, 62, E016240126410AE9, 3, 6
2022-10-05, 08:00:22, 63, E01624012641A4B3, 3, 7
2022-10-05, 08:00:22, 66, E01624012641AD7, 2, 6
2022-10-05, 08:00:22, 66, E016240126410618, 2, 6
2022-10-05, 08:00:22, 67, E016240126416A66, 2, 7
e
Male
Female
Young male
Aged male
n=4
n=8
n=15/16
n=16
Transponder Inplantation
IntelliProfiler Aanalysis
Males
Females
Young males
Aged males
Young father derived offspring (YFO)
Aged father derived offspring (AFO)
Day
3 Days
2 Days
P49 (7W)
P56 (8W)
P58
P59
P364 (52W)
P371 (53W)
P374

Fig. 2.

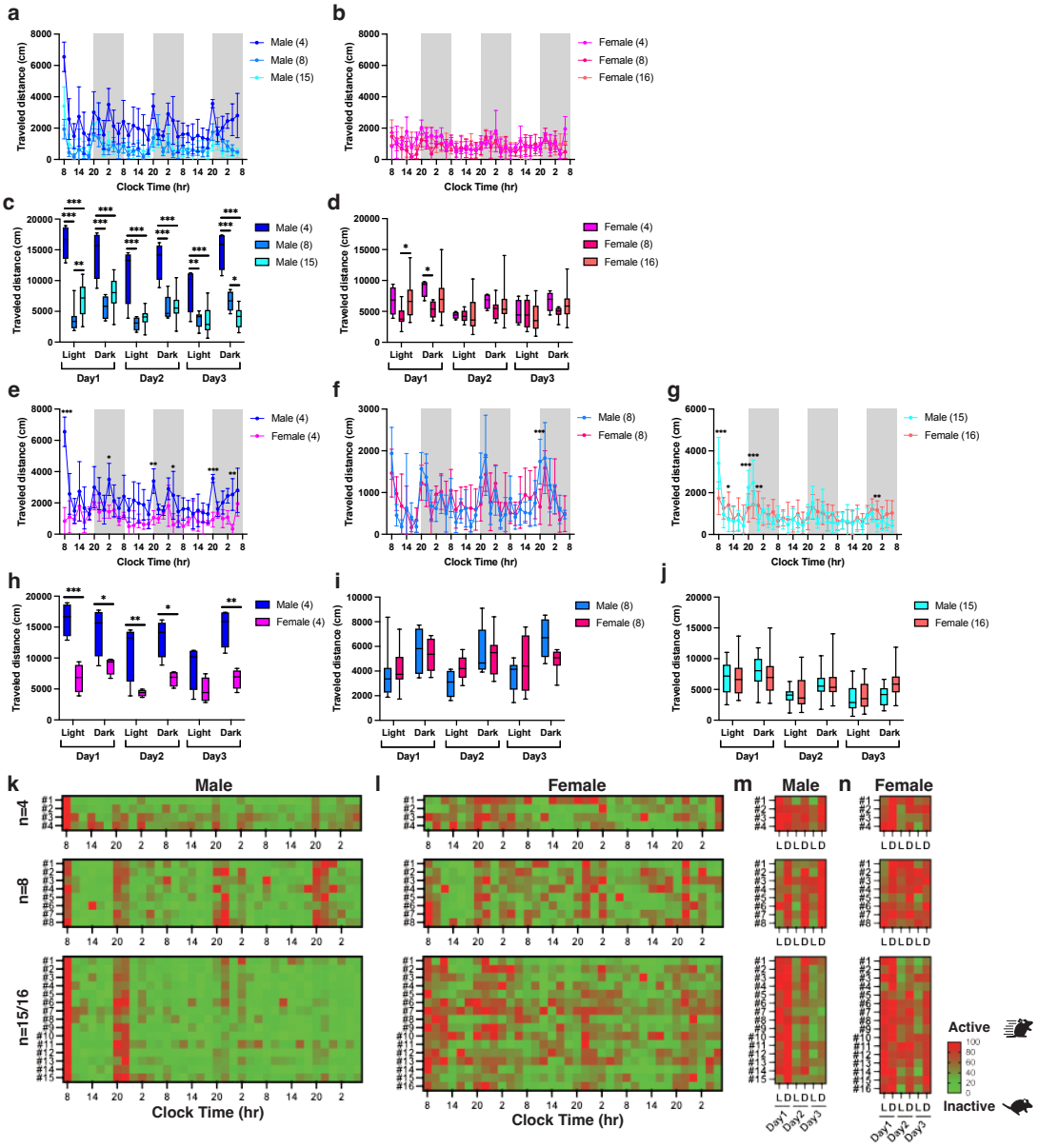
a
Traveled distance (cm)
Clock Time (hr)
Male (4)
Male (8)
Male (15)
b
Female (4)
Female (8)
Female (16)
c
Light
Dark
Day1
Day2
Day3
d
e
Male (4)
Female (4)
f
Male (8)
Female (8)
g
Male (15)
Female (16)
h
i
j
k
Male
n=4
n=8
n=15/16
l
Female
m
Male
n
Female
L D L D L D
Active
Inactive

Fig. 3.

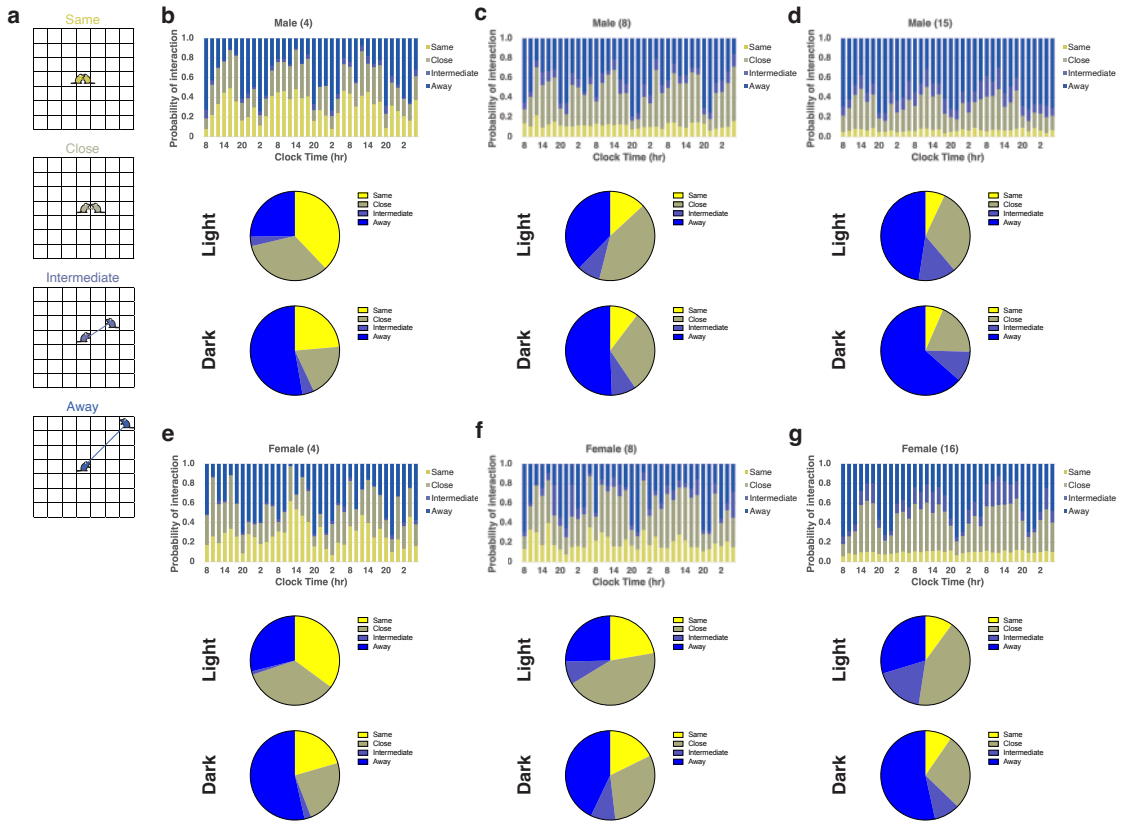
a
Same
Close
Intermediate
Away
b
Male (4)
c
Male (8)
d
Male (15)
e
Female (4)
f
Female (8)
g
Female (16)
Probability of interaction
Clock Time (hr)
Same
Close
Intermediate
Away
Light
Dark

Fig. 4.

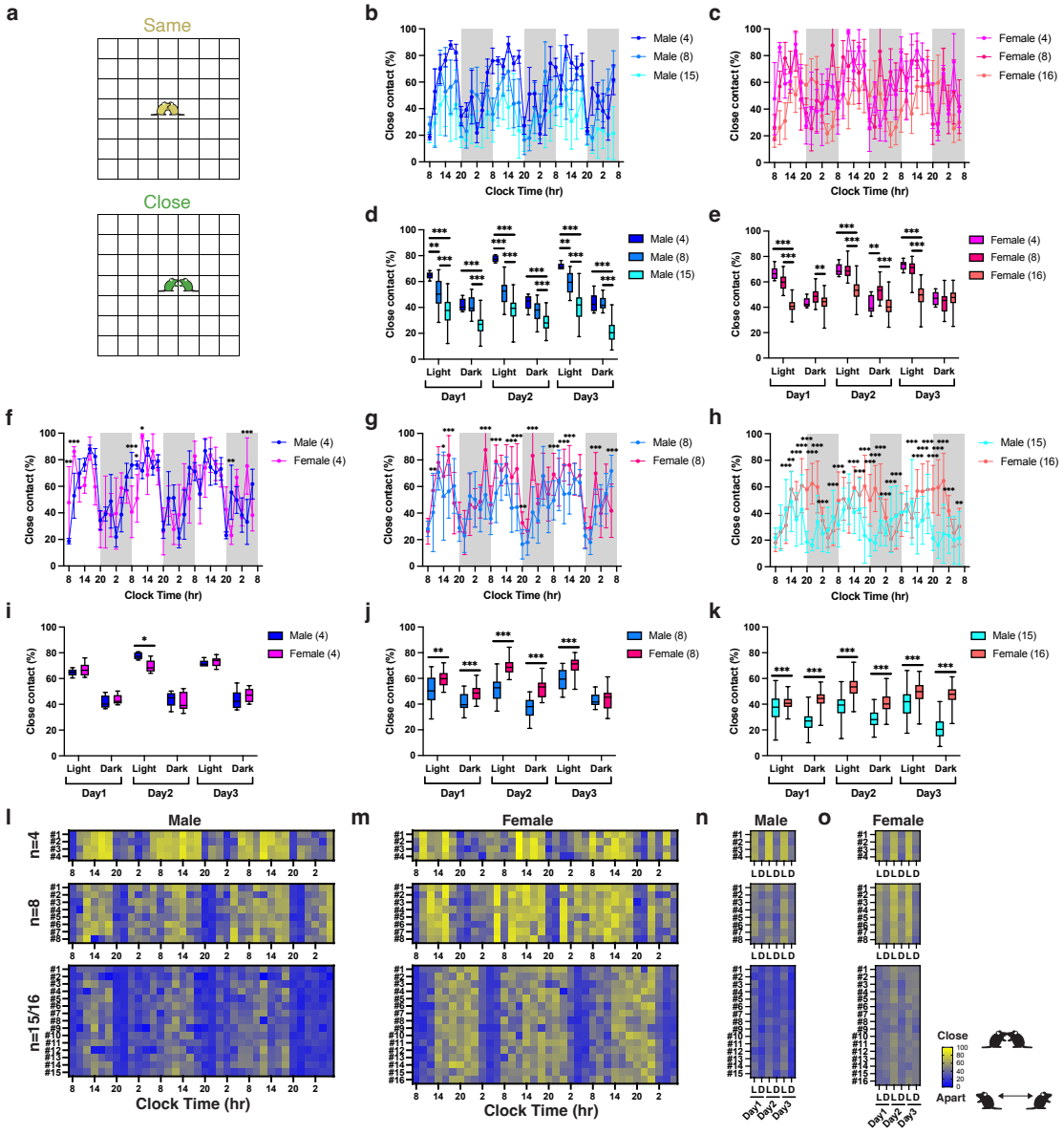
a
Same
Close
b
Male (4)
Male (8)
Male (15)
Close contact (%)
Clock Time (hr)
c
Female (4)
Female (8)
Female (16)
d
Light
Dark
Day1
Day2
Day3
e
f
Male (4)
Female (4)
g
Male (8)
Female (8)
h
Male (15)
Female (16)
i
j
k
l
Male
n=4
n=8
n=15/16
m
Female
n
o
Close
Apart

Fig. 5.

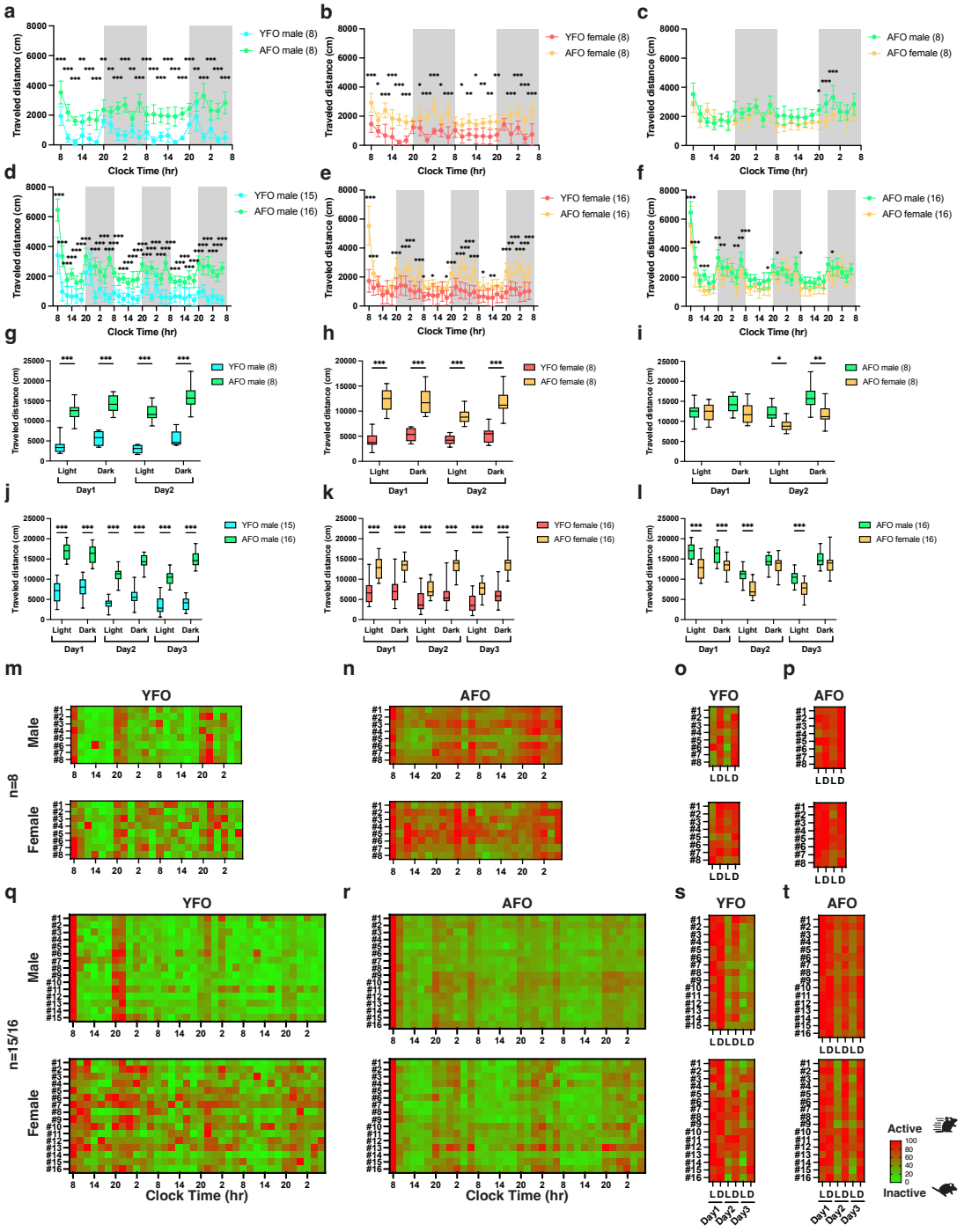
a
b
c
d
e
f
g
h
i
j
k
l
m
n
o
p
q
r
s
t
Traveled distance (cm)
Clock Time (hr)
YFO male (8)
AFO male (8)
YFO female (8)
AFO female (8)
YFO male (15)
AFO male (16)
YFO female (16)
AFO female (16)
Light
Dark
Day1
Day2
Day3
YFO
AFO
Male
Female
n=8
n=15/16
LDLD
LDLDLD
Active
Inactive

Fig. 6.

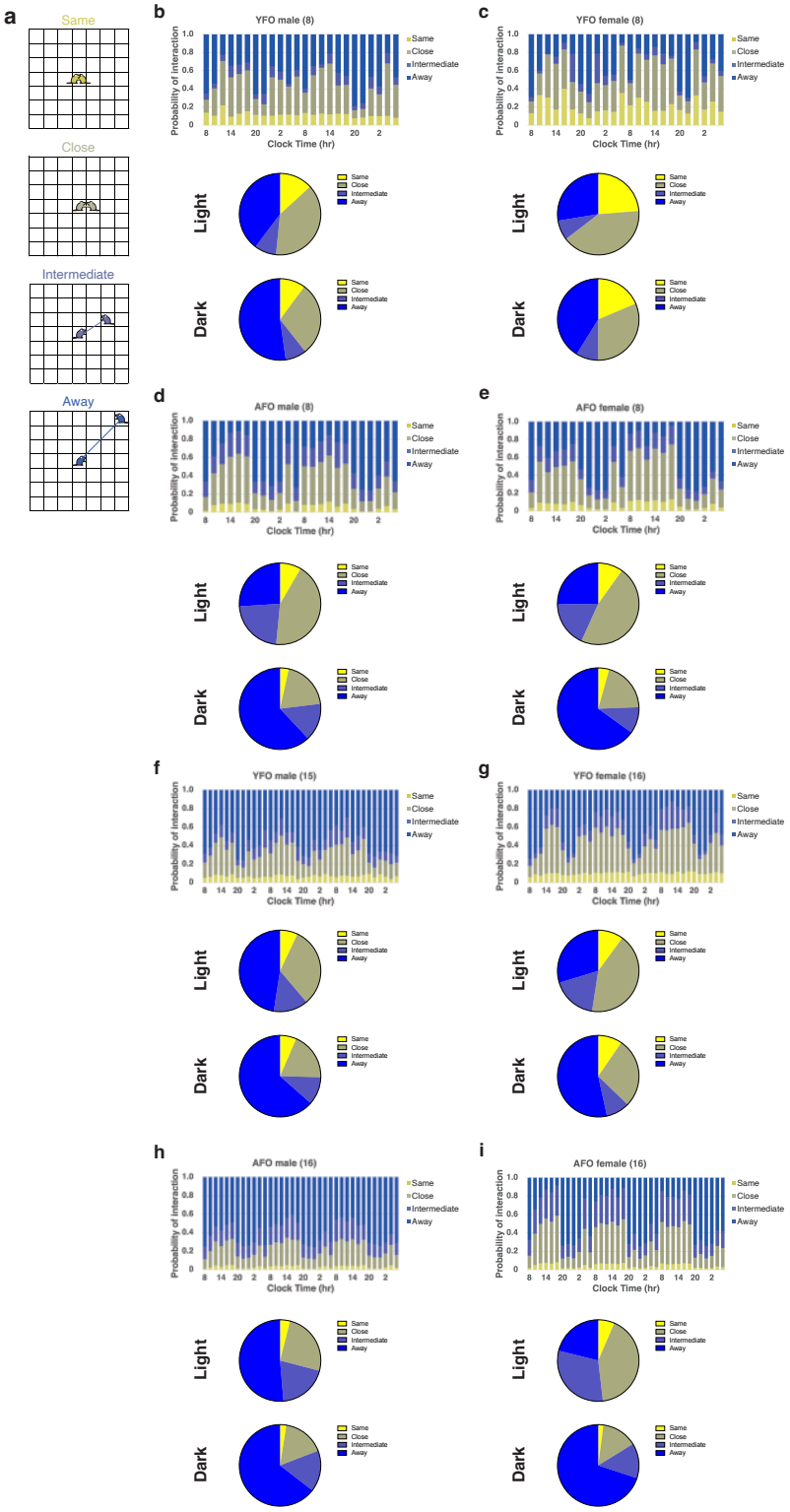
a
Same
Close
Intermediate
Away
b
YFO male (8)
c
YFO female (8)
d
AFO male (8)
e
AFO female (8)
f
YFO male (15)
g
YFO female (16)
h
AFO male (16)
i
AFO female (16)
Probability of Interaction
Clock Time (hr)
Same
Close
Intermediate
Away
Light
Dark

Fig. 7.

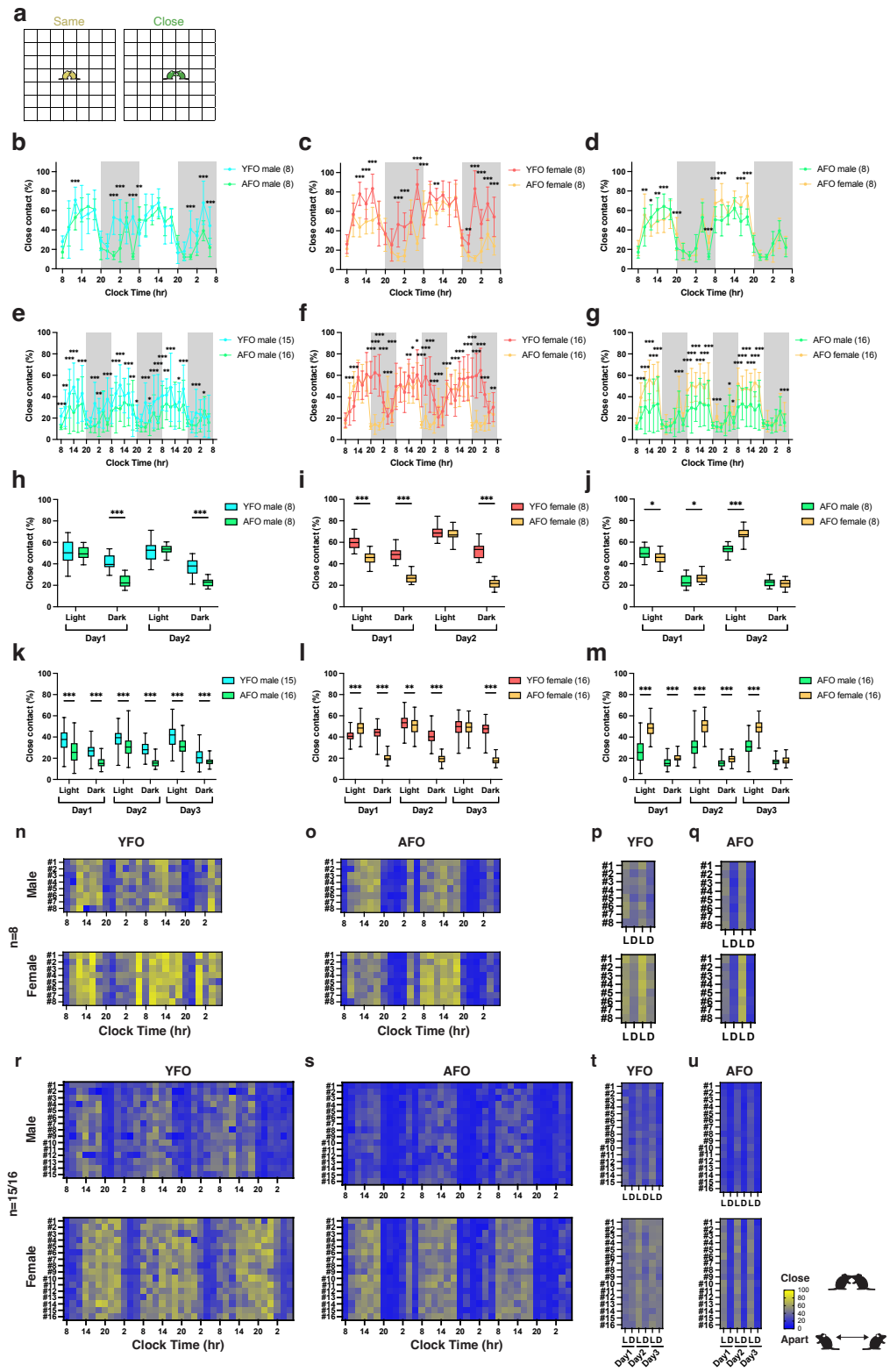
a
Same
Close
b
YFO male (8)
AFO male (8)
c
YFO female (8)
AFO female (8)
d
AFO male (8)
AFO female (8)
e
YFO male (15)
AFO male (16)
f
YFO female (16)
AFO female (16)
g
AFO male (16)
AFO female (16)
Close contact (%)
Clock Time (hr)
h
i
j
k
l
m
Light
Dark
Day1
Day2
Day3
n
o
p
q
r
s
t
u
YFO
AFO
Male
Female
n=8
n=15/16
L D L D
Close
Apart

Fig. 8.

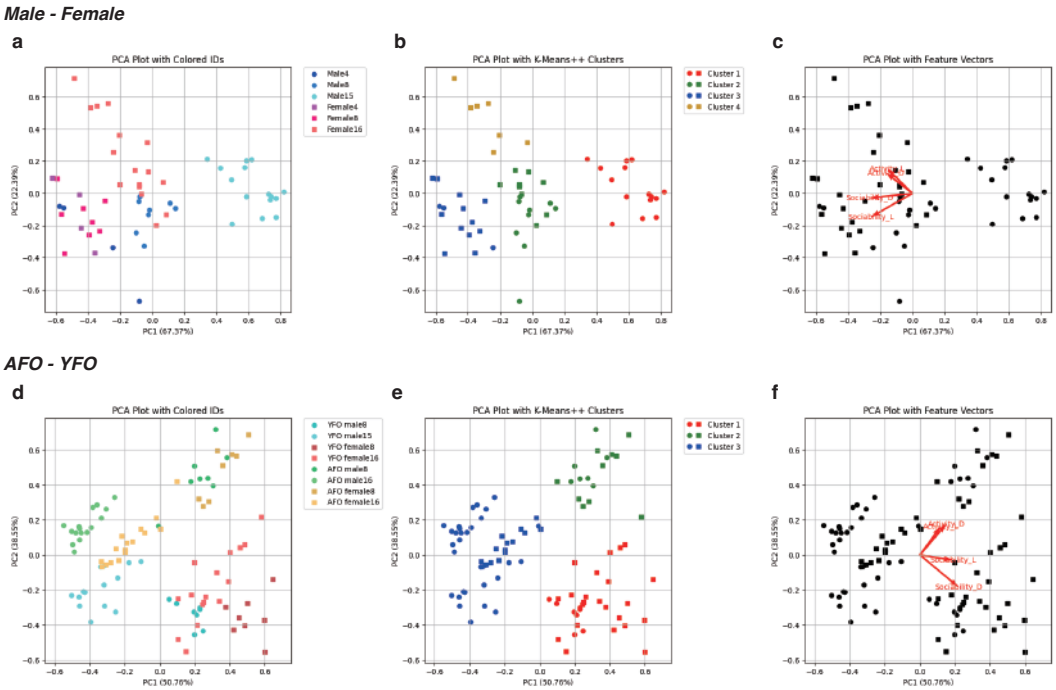
Male - Female
a
PCA Plot with Colored IDs
Male4
Male8
Male15
Female4
Female8
Female16
PC1 (67.37%)
PC2 (22.39%)
b
PCA Plot with K-Means++ Clusters
Cluster 1
Cluster 2
Cluster 3
Cluster 4
PC1 (67.37%)
PC2 (22.39%)
c
PCA Plot with Feature Vectors
PC1 (67.37%)
PC2 (22.39%)
AFO - YFO
d
PCA Plot with Colored IDs
YFO male8
YFO male15
YFO female8
YFO female16
AFO male8
AFO male16
AFO female8
AFO female16
PC1 (50.76%)
PC2 (38.55%)
e
PCA Plot with K-Means++ Clusters
Cluster 1
Cluster 2
Cluster 3
PC1 (50.76%)
PC2 (38.55%)
f
PCA Plot with Feature Vectors
PC1 (50.76%)
PC2 (38.55%)

Fig. 9.

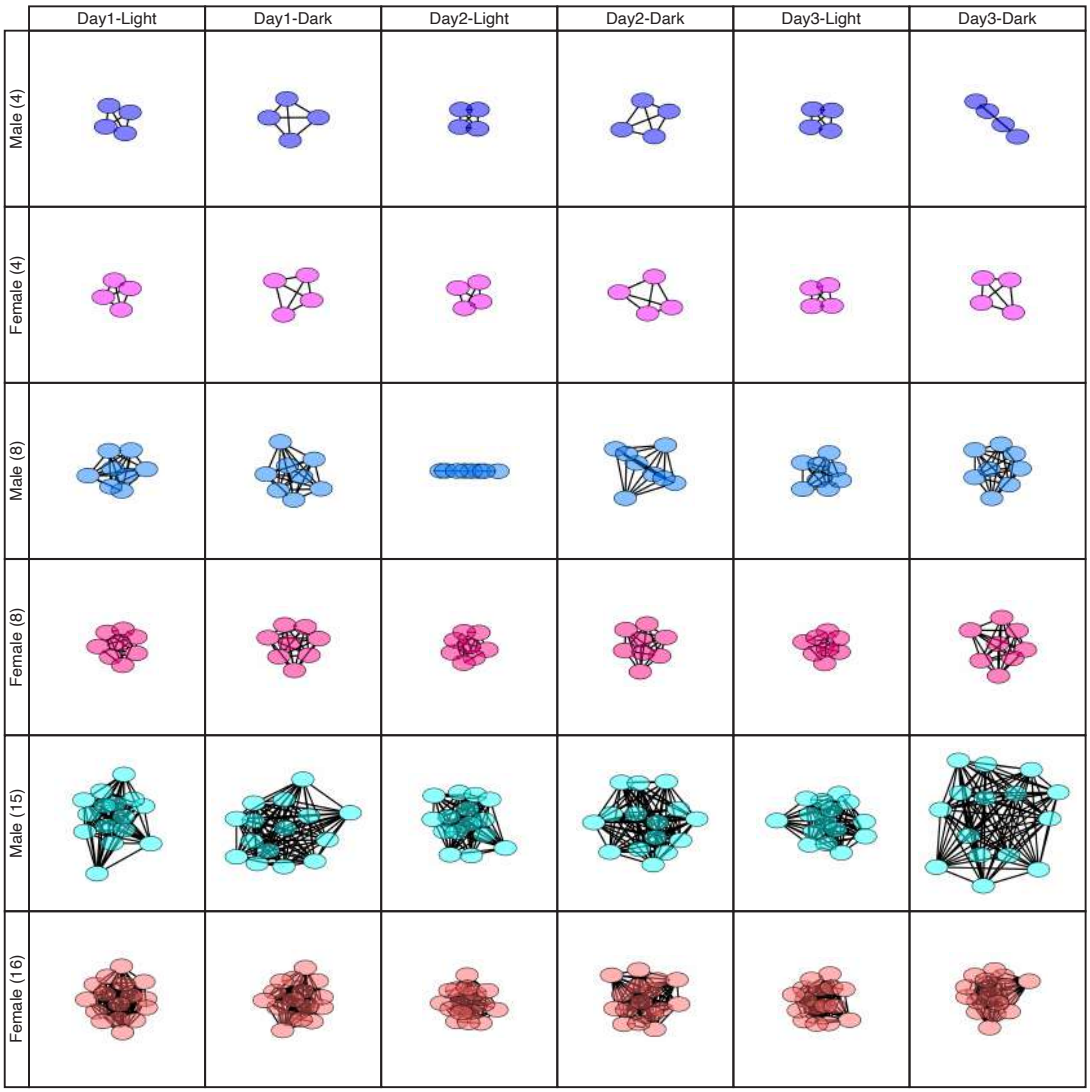
Day1-Light
Day1-Dark
Day2-Light
Day2-Dark
Day3-Light
Day3-Dark
Male (4)
Female (4)
Male (8)
Female (8)
Male (15)
Female (16)

Fig. 10.

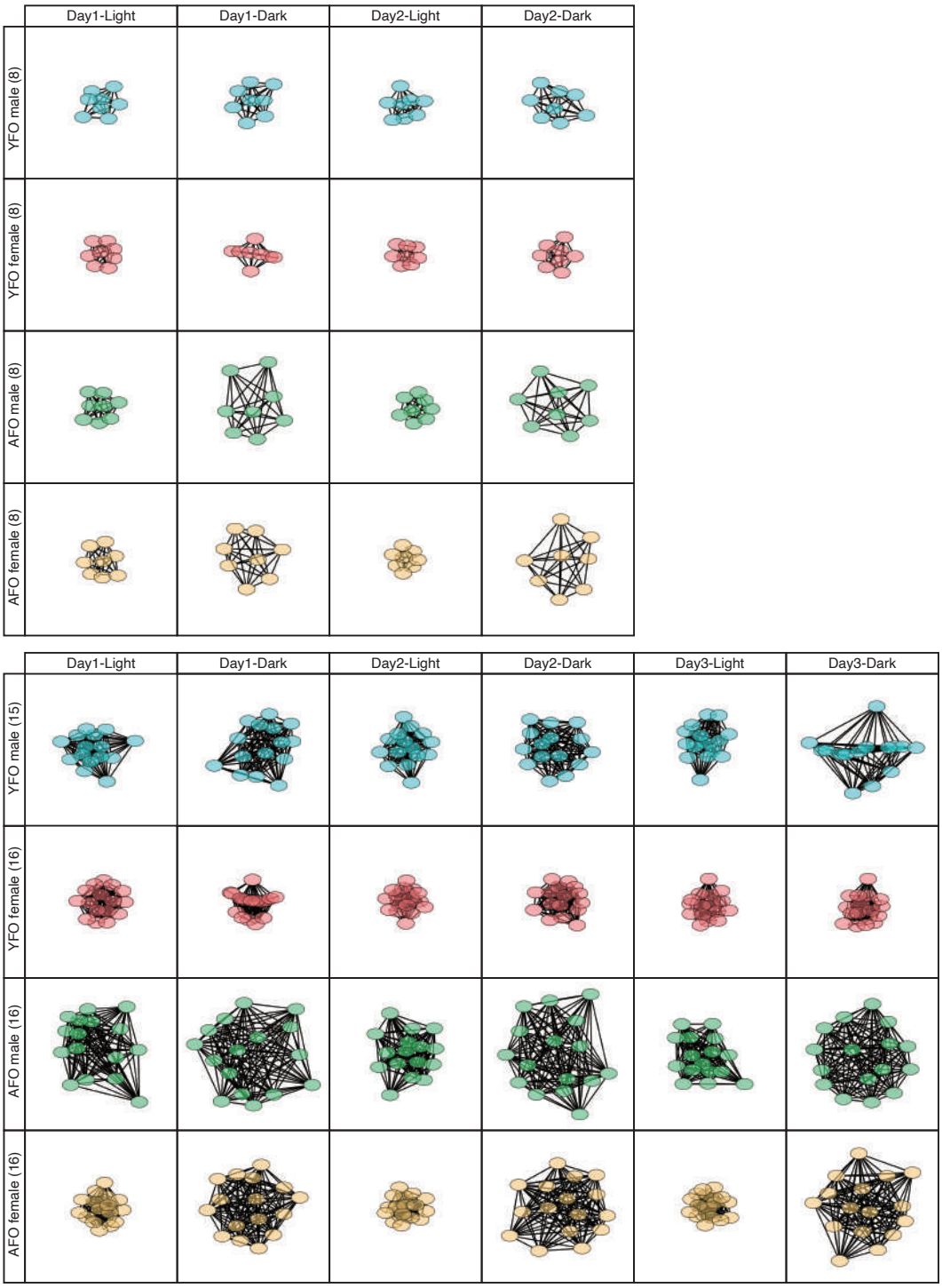
Day1-Light
Day1-Dark
Day2-Light
Day2-Dark
YFO male (8)
YFO female (8)
AFO male (8)
AFO female (8)
Day1-Light
Day1-Dark
Day2-Light
Day2-Dark
Day3-Light
Day3-Dark
YFO male (15)
YFO female (16)
AFO male (16)
AFO female (16)